THE JOURNAL OF BIOLOGICAL CHEMISTRY VOL. 288, NO. 43, pp. 30832–30842, October 25, 2013
© 2013 by The American Society for Biochemistry and Molecular Biology, Inc. Published in the U.S.A.

Histone H2A Ubiquitination Inhibits the Enzymatic Activity of H3 Lysine 36 Methyltransferases*

Received for publication, April 8, 2013, and in revised form, September 5, 2013 Published, JBC Papers in Press, September 9, 2013, DOI 10.1074/jbc.M113.475996

Gang Yuan[‡§], Ben Ma[§], Wen Yuan[§], Zhuqiang Zhang[§], Ping Chen[¶], Xiaojun Ding[§], Li Feng[§], Xiaohua Shen[‖], She Chen[§], Guohong Li[¶], and Bing Zhu[§1]

From the [‡]College of Life Sciences, Beijing Normal University, Beijing, 100875, the [§]National Institute of Biological Sciences, Beijing, 102206, the [¶]National Laboratory of Biomacromolecules, Institute of Biophysics, Chinese Academy of Sciences, Beijing 100101, and the [‖]Tsinghua-Peking Center for Life Sciences, Tsinghua University, Beijing 100084, China

Background: H3K36 methylation antagonizes Polycomb function, but it is not clear whether the reverse is true.
Results: H3K36-specific histone methyltransferases display poor enzymatic activities on nucleosome substrates containing H2A ubiquitination, an important Polycomb modification.
Conclusion: H3K36-specific histone methyltransferases can respond to chromatin environment.
Significance: It provides additional understanding about interplays among chromatin modifications and their roles in transcription regulation.

Histone H3 lysine 27 (H3K27) methylation and H2A monoubiquitination (ubH2A) are two closely related histone modifications that regulate Polycomb silencing. Previous studies reported that H3K27 trimethylation (H3K27me3) rarely coexists with H3K36 di- or tri-methylation (H3K36me2/3) on the same histone H3 tails, which is partially controlled by the direct inhibition of the enzymatic activity of H3K27-specific methyltransferase PRC2. By contrast, H3K27 methylation does not affect the catalytic activity of H3K36-specific methyltransferases, suggesting other Polycomb mechanism(s) may negatively regulate the H3K36-specific methyltransferase(s). In this study, we established a simple protocol to purify milligram quantities of ubH2A from mammalian cells, which were used to reconstitute nucleosome substrates with fully ubiquitinated H2A. A number of histone methyltransferases were then tested on these nucleosome substrates. Notably, all of the H3K36-specific methyltransferases, including ASH1L, HYPB, NSD1, and NSD2 were inhibited by ubH2A, whereas the other histone methyltransferases, including PRC2, G9a, and Pr-Set7 were not affected by ubH2A. Together with previous reports, these findings collectively explain the mutual repulsion of H3K36me2/3 and Polycomb modifications.

The eukaryotic genome is organized into chromatin, the natural substrate of nearly all biological processes that rely on DNA templates, including transcription, replication, and DNA repair (1–5). Histone proteins are important components of chromatin and can be extensively modified (1–4). Histone modifications regulate these biological processes by altering the chromatin structure and/or recruiting effector proteins, such as histone readers, that recognize these modifications (1, 6).

H3K36 methylation generally accompanies active transcription, and recent progress has shed light on the roles of H3K36 methylation in alternative splicing, dosage compensation, DNA replication, and repair (7, 8). In budding yeast, Set2 is the sole H3K36-specific methyltransferase (9). In higher eukaryotes, several enzymes have been reported to be H3K36-specific methyltransferases (7), including HYPB, which is the primary H3K36-specific trimethylase (10–12), and NSD1, NSD2, NSD3, and ASH1L, which are best characterized as H3K36-specific dimethylases (13–19).

Ubiquitinated H2A (ubH2A)[2] accounts for ~10% of the total H2A protein in human cells (20). The majority of H2A monoubiquitination occurs at a single histone H2A residue, lysine 119 (21). Ring1b in the PRC1 complex (Polycomb repressive complex 1) is the major E3 ligase that mediates H2A monoubiquitination (22, 23). Notably, Ring1b containing protein complexes interact with the Kdm2 family histone H3K36 demethylases (24–27). In addition to Ring1b, 2A-HUB (28) and BRCA1 (29) have also been reported to possess E3 ligase activity that mediates the formation of ubH2A. So far, ubH2A is best known for its function in Polycomb silencing (22, 30). More recently, ubH2A has also been suggested to play a role in repressing satellite DNA repeats (31).

In addition to PRC1, PRC2 (Polycomb repressive complex 2), the primary H3K27 methyltransferase, is another key regulator of Polycomb function (32–35). Genome-wide localization studies revealed that PRC2-mediated H3K27 methylation and PRC1-mediated H2A monoubiquitination often act cooperatively on their common target genes (36, 37).

We, and others, have previously reported that H3K36 methylation rarely coexists with H3K27me3 on the same H3 polypeptides (19, 38), suggesting that these two modifications may antagonize each other. Indeed, the catalytic activity of PRC2 is inhibited in *cis* by di- or tri-methylation at lysine 36 of the same H3 histones (19, 39, 40). However, H3K27me3 does not inhibit

* This work was supported by Chinese Ministry of Science and Technology Grants 2011CB812700 and 2011CB965300 (to B. Z.) and the Howard Hughes Medical Institute International Early Career Scientist Program (to B. Z.).
[1] To whom correspondence should be addressed. Tel.: 86-10-80728458; Fax: 86-10-80715648; E-mail: zhubing@nibs.ac.cn.

[2] The abbreviations used are: ubH2A, H2A monoubiquitination; rON, recombinant oligonucleosome; PRC, Polycomb repressive complex.

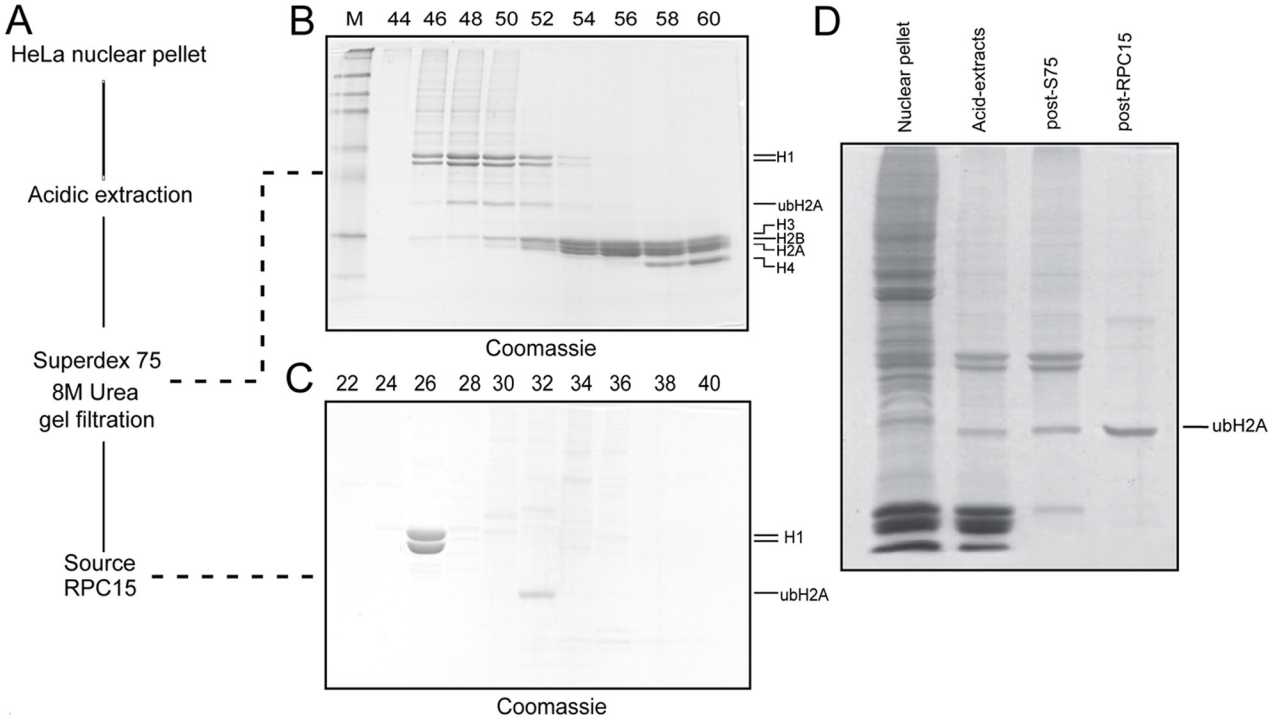

E

Purification Stage	Estimated ubH2A Purity	Impurity Removed during this step
Nuclear Pellet (Starting material)	<0.2%	–
Acid Extracts	~1.5%	Non-histone proteins
Post-Superdex 75 chromatography	~15%	H2B, H2A, H4 and most H3
Post-Source RPC15 chromatography	>95%	H1, remaining H3

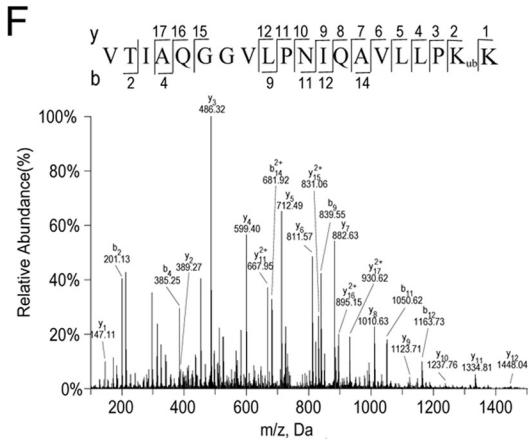

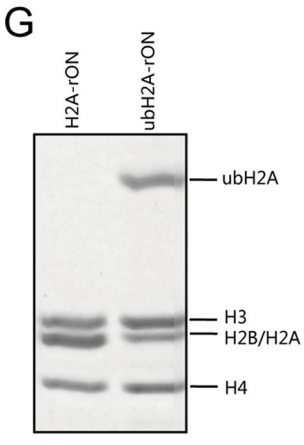

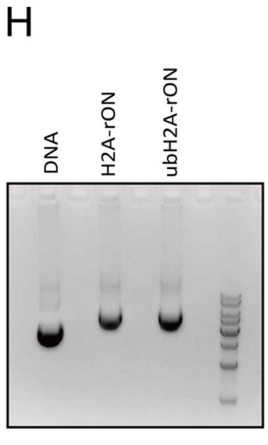

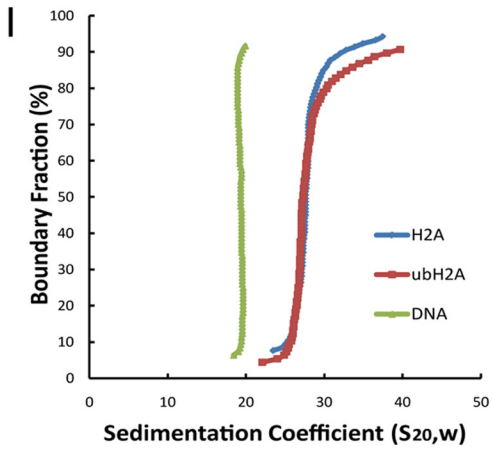

FIGURE 1. **Purification of the ubH2A protein from HeLa S3 cells.** *A*, the experimental purification scheme. *B,* Coomassie Blue staining of an SDS-PAGE gel containing fractions from the Superdex 75 chromatography. The *numbers on the top* indicate the fraction numbers. *C*, Coomassie Blue staining of an SDS-PAGE gel containing fractions from the Source RPC15 chromatography. *D,* Coomassie Blue staining of an SDS-PAGE gel containing samples at each purification stage. *E*, summary table indicating the purity of samples at each stage and the main impurities removed during each purification stage. *F*, the tandem mass spectrum of the signature peptide containing an ubiquitin moiety at lysine 119 of H2A derived from the purified ubH2A. *G*, assembled H2A- and ubH2A-containing oligonucleosomes (H2A-rON and ubH2A-rON) for subsequent assays. *H,* an agarose gel containing H2A-rON and ubH2A-rON. *I,* analytical ultracentrifugation results for H2A- and ubH2A-containing oligonucleosomes.

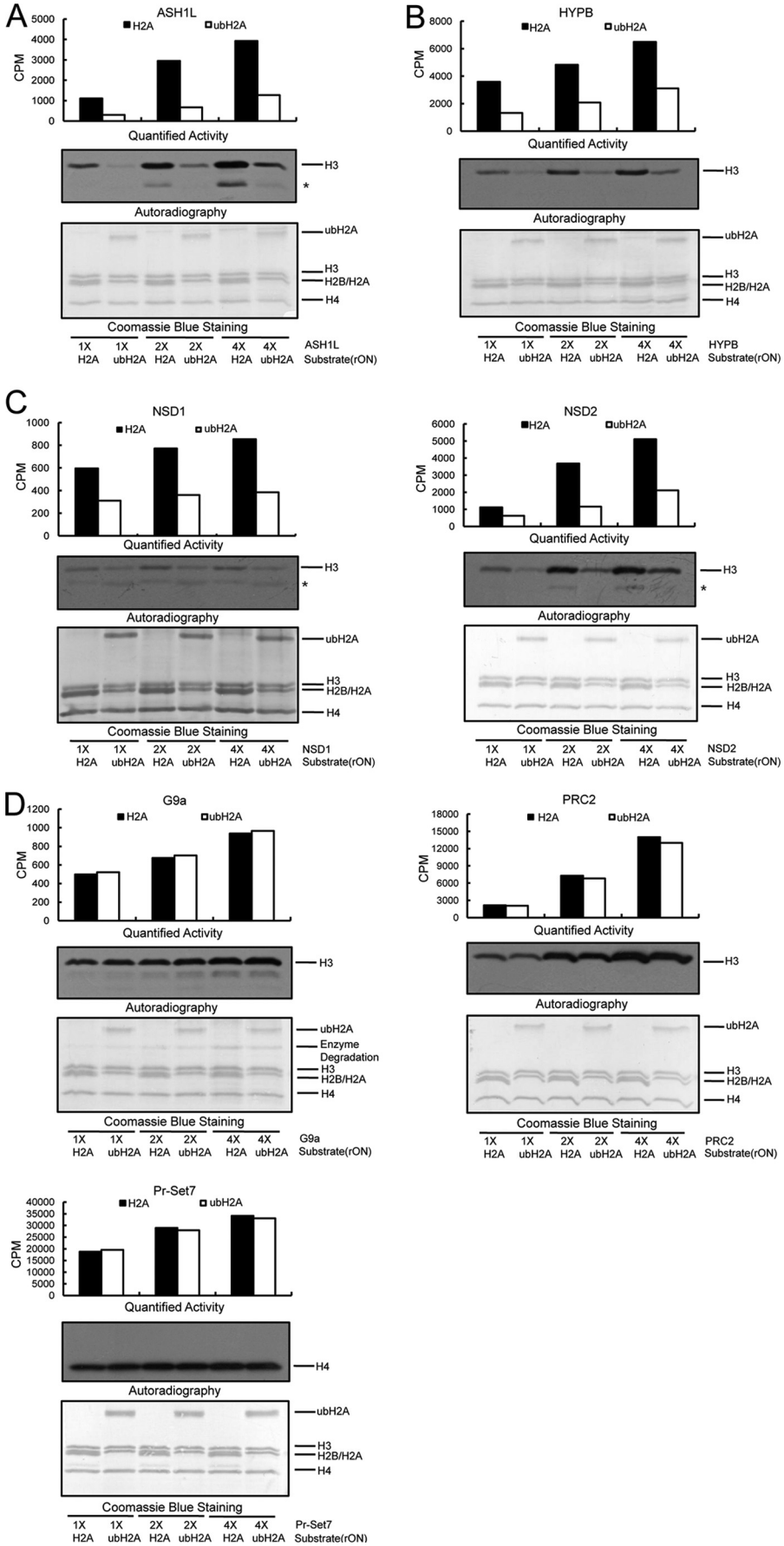
A
ASH1L
H2A
ubH2A
CPM
Quantified Activity
H3
*
Autoradiography
ubH2A
H3
H2B/H2A
H4
Coomassie Blue Staining
1X H2A
1X ubH2A
2X H2A
2X ubH2A
4X H2A
4X ubH2A
ASH1L Substrate(rON)
B
HYPB
H2A
ubH2A
CPM
Quantified Activity
H3
Autoradiography
ubH2A
H3
H2B/H2A
H4
Coomassie Blue Staining
1X H2A
1X ubH2A
2X H2A
2X ubH2A
4X H2A
4X ubH2A
HYPB Substrate(rON)
C
NSD1
H2A
ubH2A
CPM
Quantified Activity
H3
*
Autoradiography
ubH2A
H3
H2B/H2A
H4
Coomassie Blue Staining
1X H2A
1X ubH2A
2X H2A
2X ubH2A
4X H2A
4X ubH2A
NSD1 Substrate(rON)
NSD2
H2A
ubH2A
CPM
Quantified Activity
H3
*
Autoradiography
ubH2A
H3
H2B/H2A
H4
Coomassie Blue Staining
1X H2A
1X ubH2A
2X H2A
2X ubH2A
4X H2A
4X ubH2A
NSD2 Substrate(rON)
D
G9a
H2A
ubH2A
CPM
Quantified Activity
H3
Autoradiography
ubH2A
Enzyme Degradation
H3
H2B/H2A
H4
Coomassie Blue Staining
1X H2A
1X ubH2A
2X H2A
2X ubH2A
4X H2A
4X ubH2A
G9a Substrate(rON)
PRC2
H2A
ubH2A
CPM
Quantified Activity
H3
Autoradiography
ubH2A
H3
H2B/H2A
H4
Coomassie Blue Staining
1X H2A
1X ubH2A
2X H2A
2X ubH2A
4X H2A
4X ubH2A
PRC2 Substrate(rON)
Pr-Set7
H2A
ubH2A
CPM
Quantified Activity
H4
Autoradiography
ubH2A
H3
H2B/H2A
H4
Coomassie Blue Staining
1X H2A
1X ubH2A
2X H2A
2X ubH2A
4X H2A
4X ubH2A
Pr-Set7 Substrate(rON)

the enzymatic activities of H3K36-specific methyltransferases, such as HYPB and ASH1L (19). Therefore, the question remains as to whether the other known Polycomb modification, ubH2A, can antagonize H3K36 methylation. To test this possibility biochemically, milligram quantities of homogenously ubiquitinated H2A are required to assemble nucleosome substrates with fully ubiquitinated H2A.

Here we established a simple three-step protocol to purify milligram quantities of ubH2A to homogeneity from mammalian cells. We tested the enzymatic activity of several histone methyltransferases on nucleosomes assembled with ubiquitinated histone H2A. Notably, ubH2A specifically inhibits the enzymatic activities of the H3K36-specific methyltransferases including ASH1L, NSD1, NSD2, and HYPB. Together with previous reports that H3K36 methylation antagonizes Polycomb function (19, 39, 40), and the observation that E3 ligase complexes for H2A monoubiquitination associate with the Kdm2 family of H3K36 demethylases (24–27), this study helps to establish a reciprocal inhibition mechanism between H3K36 methylation and Polycomb modifications.

EXPERIMENTAL PROCEDURES

Histone Methyltransferases—Full-length recombinant histone methyltransferases or their SET domain containing fragments were expressed and purified from *Escherichia coli*, including human ASH1L (NP_060959, amino acids 2040–2716), HYPB/KMT3a (NP_054878, amino acids 1398–1704), NSD1/KMT3b (NP_071900, amino acids 1852–2082), NSD2 (NP_579877, amino acids 941–1240), Pr-Set7/Set8/KMT5a (ADP08984, full-length), and mouse G9a/KMT1c (NP_671493, amino acids 563–1172). Full-length recombinant mouse PRC2 full-length complex was expressed and purified from insect cells using the Baculovirus system.

Purification of Milligram Quantities of ubH2A—Total histone samples were isolated from HeLa S3 cells using the acid extraction method as previously reported (41). The histone samples were dissolved in denaturing buffer containing 6 M urea and 1 mM Tris-HCl (pH 3.0). The acid-extracted histones were then subjected to gel filtration over a Superdex 75 (GE Healthcare) size exclusion column in denaturing buffer containing 6 M urea and 1 mM Tris-HCl (pH 3.0) to separate ubH2A proteins from the majority of core histones, particularly the non-ubiquitinated form of H2A histones. The fractions containing ubH2A but trace amounts of non-ubiquitinated H2A histones were pooled and dialyzed against Buffer A (5% acetonitrile and 0.1% trifluoroacetic acid). The dialyzed samples were then loaded onto a Source RPC15 hydrophobicity column (Sigma), and the impurities were separated from the ubH2A with a linear gradient of Buffer A to Buffer B (90% acetonitrile and 0.1% trifluoroacetic acid) in 5 column volumes. Fractions containing the pure ubH2A were pooled for further analysis.

Mass Spectrometry (MS) Analysis—The purified ubH2A proteins were analyzed by LC (liquid chromatography)-MS/MS (tandem mass spectrometry) using a QSTAR XL mass spectrometer (AB SCIEX). The LC-MS/MS experiments were performed as described previously (42, 43).

Reconstitution of Histone Octamers and Nucleosomes—Recombinant histone octamers were reconstituted by mixing equal molar of core histones or ubH2A and then dialyzing against 2 M NaCl, followed by gel filtration purification over a 24-ml Superdex 200 size exclusion column. Then we assembled oligonucleosomes with equal molar of histone octamers and pG5E4 plasmid DNA, by stepwise dialysis against 1.2, 1.0, 0.8, and 0.6 M NaCl and finally TE (10 mM Tris-HCl (pH 8.0), 1 mM EDTA) (44).

Analytical Ultracentrifugation—Sedimentation experiments were performed on a Beckman Coulter ProteomeLab XL-I using an An-60Ti rotor. Samples with an initial absorbance at 260 nm of 0.8 were equilibrated for 2 h at 20 °C under vacuum in a centrifuge prior to sedimentation. The absorbance at 260 nm was measured in a continuous scan mode during sedimentation at 32,000 × *g* in 12-mm double-sector cells. The data were analyzed using the enhanced van Holde-Weischet analysis and the Ultrascan II 9.9 revision 1504. The $s_{20,w}$ values (sedimentation coefficiency corrected for water at 20 °C) were calculated with a partial specific volume of 0.622 ml/g for oligonucleosome samples with the buffer density and viscosity adjusted.

Mononucleosome Preparation—Cells were fixed with 1% formaldehyde for 10 min at room temperature and then quenched with 125 mM glycine for 5 min. These cells were then washed with cold PBS and subjected to micrococal nuclease (MNase, TAKARA) digestion, according to the protocol described previously (19).

Immunoprecipitation—The mononucleosomes prepared in the above step were used as the input materials for the subsequent immunoprecipitation experiments. The mononucleosomes were incubated with antibodies against ubH2A (CST 8240s) or H3K36me3 (Abcam ab9050) for 3 h at 4 °C, and then captured with Protein A-agarose beads. The beads were extensively washed with buffer containing 10 mM Tris-HCl (pH 8.0), 500 mM KCl, 0.5 mM EDTA, 1 mM DTT, 10% glycerol, and 0.1% Nonidet P-40. The immunoprecipitated mononucleosomes were then eluted with SDS-PAGE loading buffer. The antibodies used for Western blotting analysis were anti-ubH2A (Millipore 05-678), anti-H3K36me2 (Millipore 07-369), anti-H3K36me3 (Abmart P30057M), anti-H3K27me3 (Millipore 07-449), anti-H3K9me2 (Active motif 39375), anti-H4K20me1 (Abcam ab9051), and anti-H3 (Millipore 07-690).

Histone Lysine Methyltransferase Assays—The histone methyltransferase assays were performed in a 30-μl reaction mixture containing 1 μl of *S*-[*methyl*-^{3}H]adenosylmethionine

FIGURE 2. **ubH2A inhibits the activity of H3K36-specific methyltransferases *in vitro*.** *A,* ubH2A inhibits ASH1L activity. *B,* ubH2A inhibits HYPB activity. *C,* ubH2A inhibits the activities of NSD1 and NSD2. *D,* ubH2A does not affect the HMT activities of G9a, PRC2, and Pr-Set7. The assays were performed with constant amounts of recombinant oligonucleosomes (1.2 μg) and increasing amounts of HMTases. ASH1L (1X, 0.8 μg; 2X, 1.6 μg; 4X, 3.2 μg); HYPB (1X, 1.0 μg; 2X, 2.0 μg; 4X, 4.0 μg); NSD1 (1X, 1.5 μg; 2X, 3.0 μg; 4X, 6.0 μg); NSD2 (1X, 0.6 μg; 2X, 1.2 μg; 4X, 2.4 μg); G9a (1X, 0.5 μg; 2X, 1.0 μg; 4X, 1.5 μg); Pr-Set7 (1X, 0.1 μg; 2X, 0.2 μg; 4X, 0.4 μg); PRC2 (1X, 0.4 μg; 2X, 0.8 μg; 4X, 1.6 μg). Please note: H2A co-migrates with H2B in H2A-containing oligonucleosome samples; therefore, the intensity of H3 and H4 histones should be used for comparing the amounts of H2A- and ubH2A-containing nucleosomes. The *asterisk* indicates an H3 degradation band present in some of the substrates.

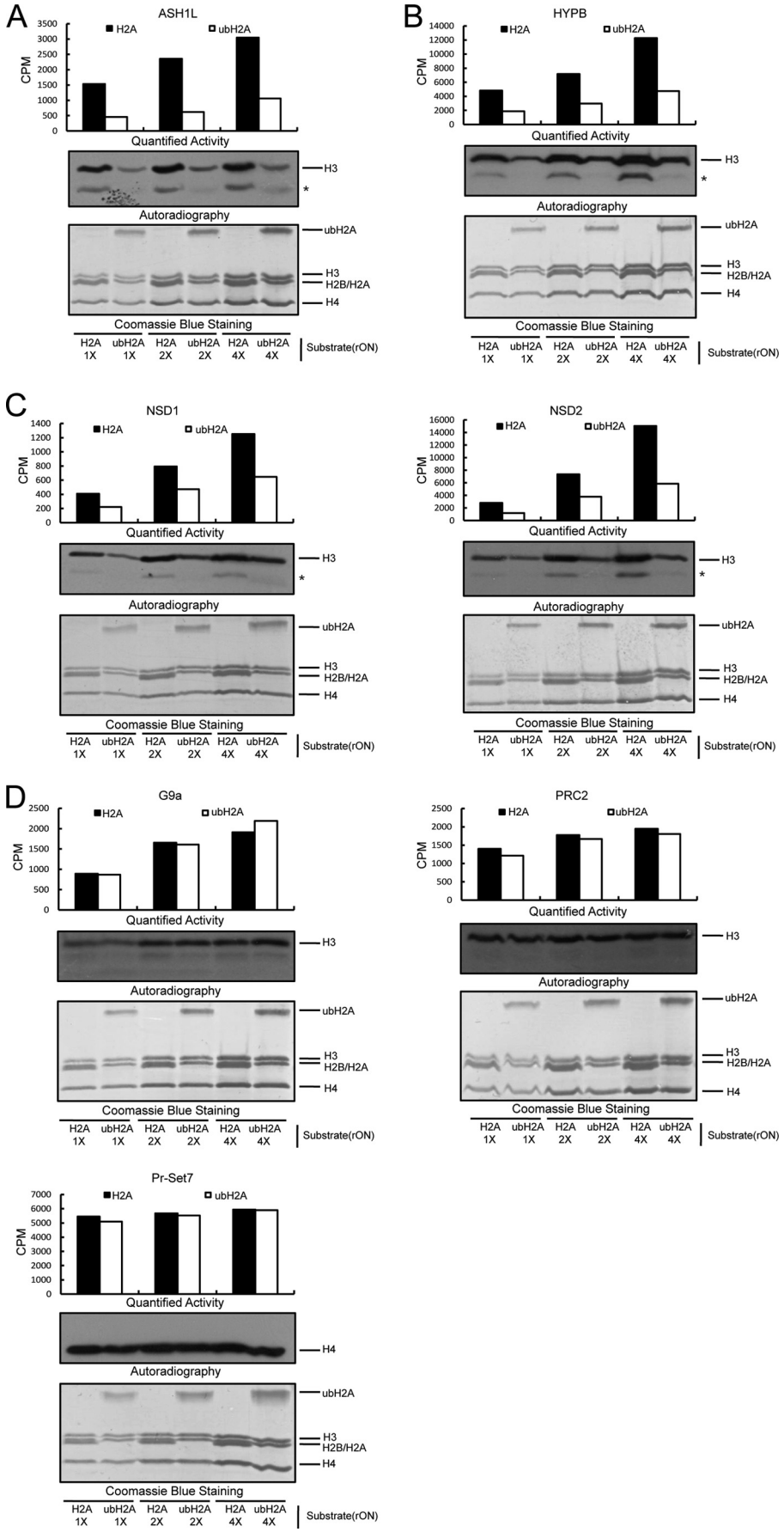
A
ASH1L
H2A
ubH2A
CPM
Quantified Activity
H3
*
Autoradiography
ubH2A
H3
H2B/H2A
H4
Coomassie Blue Staining
H2A 1X
ubH2A 1X
H2A 2X
ubH2A 2X
H2A 4X
ubH2A 4X
Substrate(rON)
B
HYPB
C
NSD1
NSD2
D
G9a
PRC2
Pr-Set7

(PerkinElmer Life Sciences, NET-155H, 0.55 μCi/μl, 78 Ci/mmol), recombinant oligonucleosomes (rON), and the corresponding enzymes in histone methyltransferase assay buffer as previously described (19, 45). The reaction products were separated by 13% SDS-PAGE, then transferred to PVDF membranes and subjected to autoradiography. For quantification, the above membranes were stained with Coomassie Blue G-250 followed by liquid scintillation counting for each stained histone band excised individually.

Histone Deubiquitination—Histone deubiquitination was performed in a 20-μl reaction mixture containing 50 mM Tris-HCl (pH 7.5), 50 mM NaCl, 5 mM DTT, 2 μg of ubH2A rON, and 1 μg of USP21 enzyme. The reaction mixture was incubated at 30 °C for 2 h. The subsequent histone methyltransferase assay was performed directly in this reaction mixture.

ChIP-Seq Data Analysis—ChIP-Seq data for ubH2A (46) and H3K36me3 (47) obtained from mouse embryonic fibroblast cells were retrieved from the NCBI SRA database under accession numbers SRP000811 and SRP000415, respectively. Raw reads were mapped to Mouse genome mm9. Uniquely mapped reads were kept and extended to average fragment size. Based on these extended reads, genome coverage was calculated and normalized to equal sequencing depth. Each gene was normalized to 0–100% according to its length. The fold-enrichment of all genes were averaged for each 1% window and plotted from 20% upstream of the transcription start sites to 20% downstream of the transcription end sites.

RESULTS

Purification of ubH2A Histone Proteins—To test the biochemical roles of ubiquitinated histones, bulk amounts of fully ubiquitinated histone substrates are often required. Fully ubiquitinated H2A and H2B have been derived with chemical reactions (48–50). However, these materials remain difficult to obtain for the majority of biologists. Because ubH2A histone proteins account for ~10% of the total H2A proteins in mammalian cells (20), to obtain pure milligram quantities of ubH2A proteins that would allow most biochemical studies to be performed, we developed a simple three-step purification strategy (Fig. 1*A*) by combining acidic extraction, previously reported denaturing gel filtration (51) (Fig. 1*B*) with reverse-phase chromatography (Fig. 1*C*). The majority of non-histone proteins were first removed by acidic extraction. Then, the H2B, H2A, H4, and the majority of H3 histones were removed by denaturing gel filtration over a Superdex 75 column. Finally, the H1 histones and residual amounts of H3 histones were removed by reverse-phase chromatography over a source RPC15 column (Fig. 1, *D* and *E*). With this protocol, we were able to obtain ~3 mg of ubH2A with >95% purity (Fig. 1*D*) from 1×10^{11} HeLa S3 cells (~100 liter suspension culture). The remaining non-histone impurities were further removed during subsequent nucleosome assembly procedures.

To confirm the identity of the purified ubH2A, the protein band (Fig. 1*D*) was excised from the SDS-PAGE gel and subjected to mass spectrometry analysis. We successfully detected the signature peptide containing a single ubiquitin moiety at lysine 119 of H2A (Fig. 1*F*). Importantly, no other core histones and modifications were detected.

We assembled recombinant histone octamers using the above purified ubH2A and recombinant human core histones purified from *E. coli*. Then we further assembled oligonucleosomes with plasmid DNA and octamers containing fully ubiquitinated H2A or regular H2A (Fig. 1*G*). Because certain histone methyltransferase, like PRC2, alters its enzymatic activity on oligonucleosomes with different density (44), oligonucleosomes containing ubH2A or regular H2A were assembled with comparable octamer/DNA ratio. Indeed, these oligonucleosomes displayed similar mobility on agarose gels (Fig. 1*H*). Moreover, analytical ultracentrifugation analysis for these two substrates indicated that more than 90% of these two oligonucleosomes share similar sedimentation coefficiency (Fig. 1*I*), which further confirms that the two substrates share similar density.

ubH2A Inhibits the Activity of H3K36 Methyltransferases in Vitro—After generating nucleosome substrates containing fully ubiquitinated H2A, we determined whether ubH2A regulates the enzymatic activity of a panel of histone methyltransferases, including PRC2, which mediates the H3K27me3 (32–35) Polycomb modification and ASH1L, which mediates H3K36me2 (17–19) and antagonizes Polycomb function (52–54).

ASH1L displayed greatly lower enzymatic activity on the nucleosomes assembled with ubH2A than on equal amounts of nucleosomes assembled with H2A (Fig. 2*A*). Interestingly, similar inhibitory effects by ubH2A were also observed for other H3K36-specific HMTases, including HYPB (Fig. 2*B*), NSD1, and NSD2 (Fig. 2*C*). Notably, the inhibitory role of ubH2A was most prominent on ASH1L (Fig. 2*A*), which may be consistent with the role of ASH1L in Polycomb regulation. By contrast, the inhibitory role of ubH2A on NSD1 was the mildest (Fig. 2*C*). This may reflect a differential regulation but may also be alternatively explained by the weakest activity of NSD1 under our test conditions, which may reduce the assay sensitivity. Importantly, the above observed negative impact of ubH2A appeared to be specific to H3K36 methyltransferases, because ubH2A had little effect on the other tested HMTases, including PRC2, G9a, and Pr-Set7 (Fig. 2*D*). All above HMT activity assays were performed under three conditions containing increasing amounts of the respective HMTases and the results were consistent with each other (Fig. 2).

We then attempted to measure the K_m and V_{max} values of these HMTases on nucleosomes containing either regular H2A or ubH2A by titrating the amounts of substrates. Unfortu-

FIGURE 3. **ubH2A inhibits the activity of H3K36-specific methyltransferases *in vitro*.** *A*, ubH2A inhibits ASH1L activity. *B*, ubH2A inhibits HYPB activity. *C*, ubH2A inhibits the activities of NSD1 and NSD2. *D*, ubH2A does not affect the HMT activities of G9a, PRC2, and Pr-Set7. The assays were performed with constant amounts of HMTases (ASH1L, 1.6 μg; HYPB, 2.0 μg; NSD1, 3.0 μg; NSD2, 1.2 μg; G9a, 1.0 μg; Pr-Set7, 0.2 μg; PRC2, 0.8 μg) and increased amounts of recombinant oligonucleosomes (1X, 0.6 μg; 2X, 1.2 μg; 4X, 2.4 μg). Please note: H2A co-migrates with H2B in H2A-containing oligonucleosome samples; therefore, the intensity of H3 and H4 histones should be used for comparing the amounts of H2A- and ubH2A-containing nucleosomes. The *asterisk* indicates an H3 degradation band present in some of the substrates.

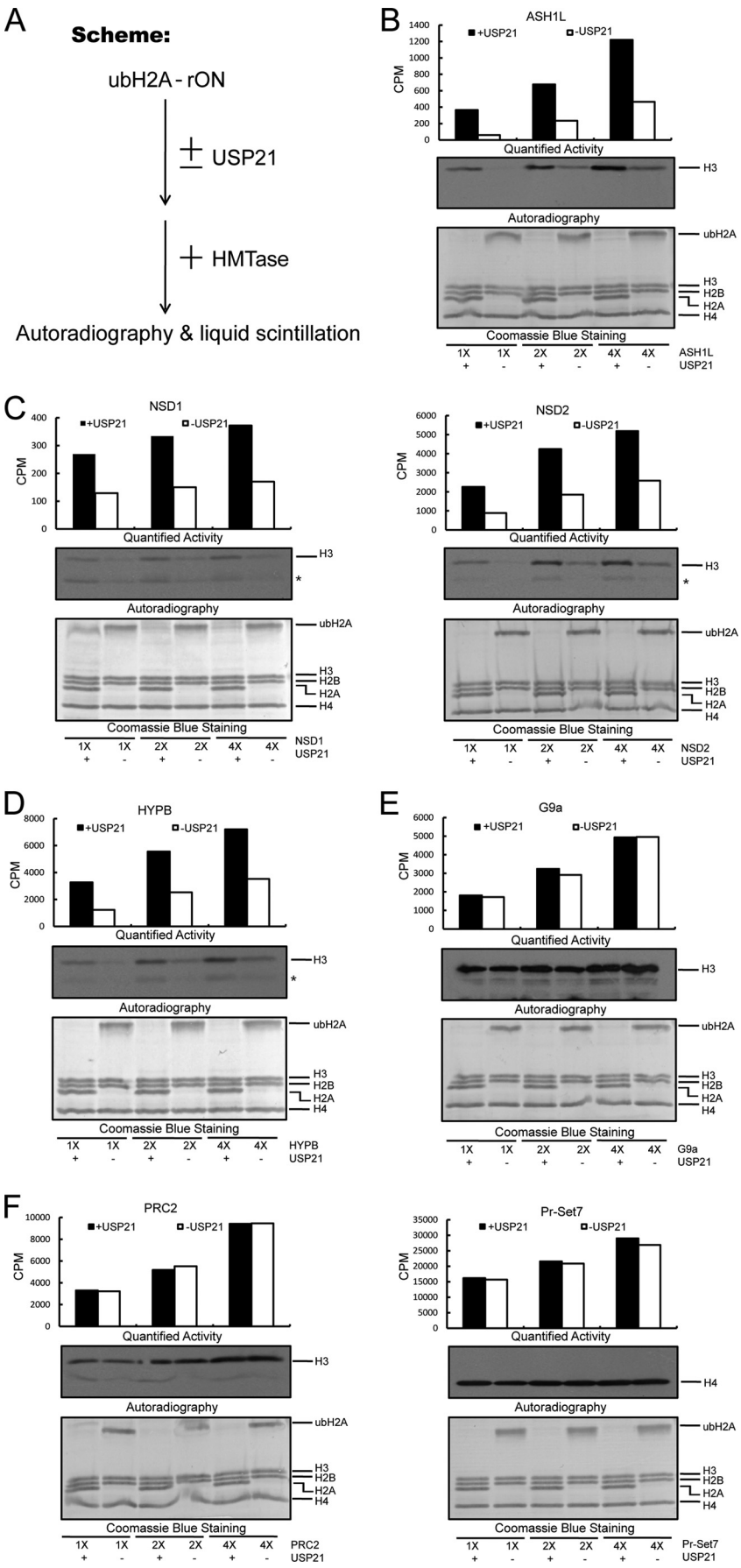
A
Scheme:
ubH2A - rON
± USP21
+ HMTase
Autoradiography & liquid scintillation
B
ASH1L
+USP21
-USP21
CPM
Quantified Activity
H3
Autoradiography
ubH2A
H3
H2B
H2A
H4
Coomassie Blue Staining
1X 1X 2X 2X 4X 4X ASH1L
+ - + - + - USP21
C
NSD1
NSD2
D
HYPB
E
G9a
F
PRC2
Pr-Set7

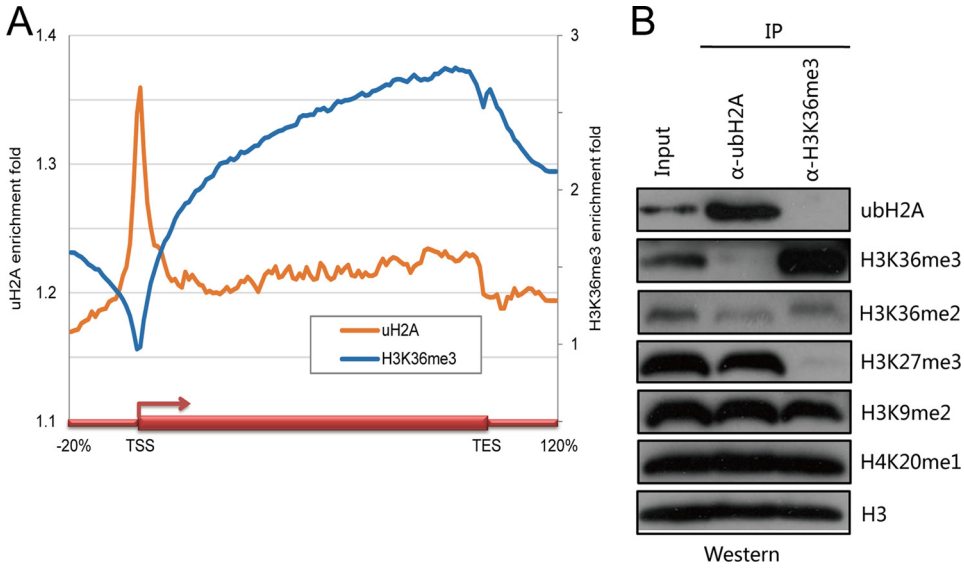

FIGURE 5. **ubH2A and H3K36me3 rarely co-exist *in vivo*.** *A,* ubH2A and H3K36me3 are distributed at distinct regions in mouse embryonic fibroblast cells based on previously published ChIP-Seq data. *B,* the immunoprecipitation experiments demonstrate that ubH2A and H3K36me3 rarely co-exist in the same mononucleosomes. *TSS*, transcription start site; *TES*, transcription end sites.

nately, the histone methyltransferase activity assay could not reach saturation with practical amounts of the substrates for several of the HMTases; therefore, accurate measurement of the K_m and V_{max} values could not be obtained. Nevertheless, we compared the histone methyltransferase activities at different substrate concentrations and observed that the H3K36-specific HMTases consistently displayed lower activities on ubH2A containing nucleosomes than regular nucleosomes at each comparable concentration (Fig. 3, *A–C*). This inhibitory effect by ubH2A was not observed on the other tested HMTases, including PRC2, G9a, and Pr-Set7 (Fig. 3*D*).

To further confirm the observed inhibitory effect on the activity of H3K36-specific HMTases was due to the ubiquitin modification, but not any other potential associated moieties, we directly compared the activity of these HMTases on ubH2A containing mononucleosomes with or without pretreatment with an ubH2A-specific deubiquitinase, USP21 (Fig. 4*A*) (55). Recombinant human USP21 expressed and purified from *E. coli* efficiently deubiquitinated ubH2A containing oligonucleosomes (Fig. 4). Pretreatment with USP21 greatly increased the enzymatic activity of H3K36-specific HMTases (Fig. 4, *B–D*), but had little effect on the other tested HMTases, including PRC2, G9a, and Pr-Set7 (Fig. 4, *E* and *F*). The above results collectively demonstrated a specific inhibitory role of ubH2A on H3K36-specific HMTases.

ubH2A and H3K36 Methylation Rarely Co-exist in Vivo—The observations that ubH2A inhibits H3K36-specific HMTases (Figs. 2–4), that ubH2A often coexist with H3K27 methylation (36, 37), and that H3K27 methylation rarely coexists with H3K36 methylation on the same H3 polypeptides (19, 38), collectively suggest that ubH2A and H3K36 methylation should have a distinct genomic distribution and that they may not frequently co-exist in mononucleosomes.

It has been well established that H3K36me2 and H3K36me3 are enriched at the coding regions of active genes (56). By contrast, ubH2A appears to be enriched at the regions surrounding transcription starting sites (46). However, these data have not previously been directly compared using genome-wide profiling data from the same type of cells before. We performed a direct comparison of published ChIP-Seq data sets for ubH2A (46) and H3K36me3 (47), both generated in mouse embryonic fibroblast cells. Indeed, these two modifications displayed distinct distribution patterns and were negatively correlated with each other (Fig. 5*A*).

To further determine whether H3K36 methylation and ubH2A co-exist at the mononucleosome level, we performed immunoprecipitation experiments with antibodies specific for ubH2A and H3K36me3. To prevent the occurrence of deubiquitination events in the lysates, the input mononucleosomes were prepared from pre-fixed cells. Anti-ubH2A antibodies clearly enriched ubH2A in the immunoprecipitated materials (Fig. 5*B*). By contrast, H3K36me3 was nearly depleted and H3K36me2 was significantly reduced (Fig. 5*B*). Consistently, mononucleosomes precipitated with anti-H3K36me3 antibodies contained enriched H3K36me3 and barely detectable ubH2A (Fig. 5*B*). Such mutual exclusion was not observed for the other tested histone modifications, including H3K9me2 and H4K20me1 (Fig. 5*B*). The above data collectively support that ubH2A and H3K36 methylation rarely co-exist *in vivo*.

FIGURE 4. **Deubiquitination of ubH2A containing oligonucleosomes prior to enzymatic activity assay stimulates the activity of H3K36-specific methyltransferases *in vitro*.** *A,* experimental scheme. *B,* removal of ubiquitin stimulates ASH1L activity. *C,* removal of ubiquitin stimulates the activities of NSD1 and NSD2. *D,* removal of ubiquitin stimulates HYPB activity. *E,* removal of ubiquitin does not affect the activity of G9a. *F,* removal of ubiquitin does not affect the activities of PRC2 and Pr-Set7. The assays were performed with constant amounts of recombinant ubH2A-rON and three different concentrations of HMTases similar to experiments described in the legend to Fig. 3. 1 μg of recombinant USP21 was used to specifically deubiquitinate ubH2A modification on rON substrates. Please note that pretreatment with USP21 converted a high molecular weight ubH2A band to a low molecular weight H2A band in the Coomassie Blue-stained membranes. The *asterisk* indicates an H3 degradation band present in some of the substrates.

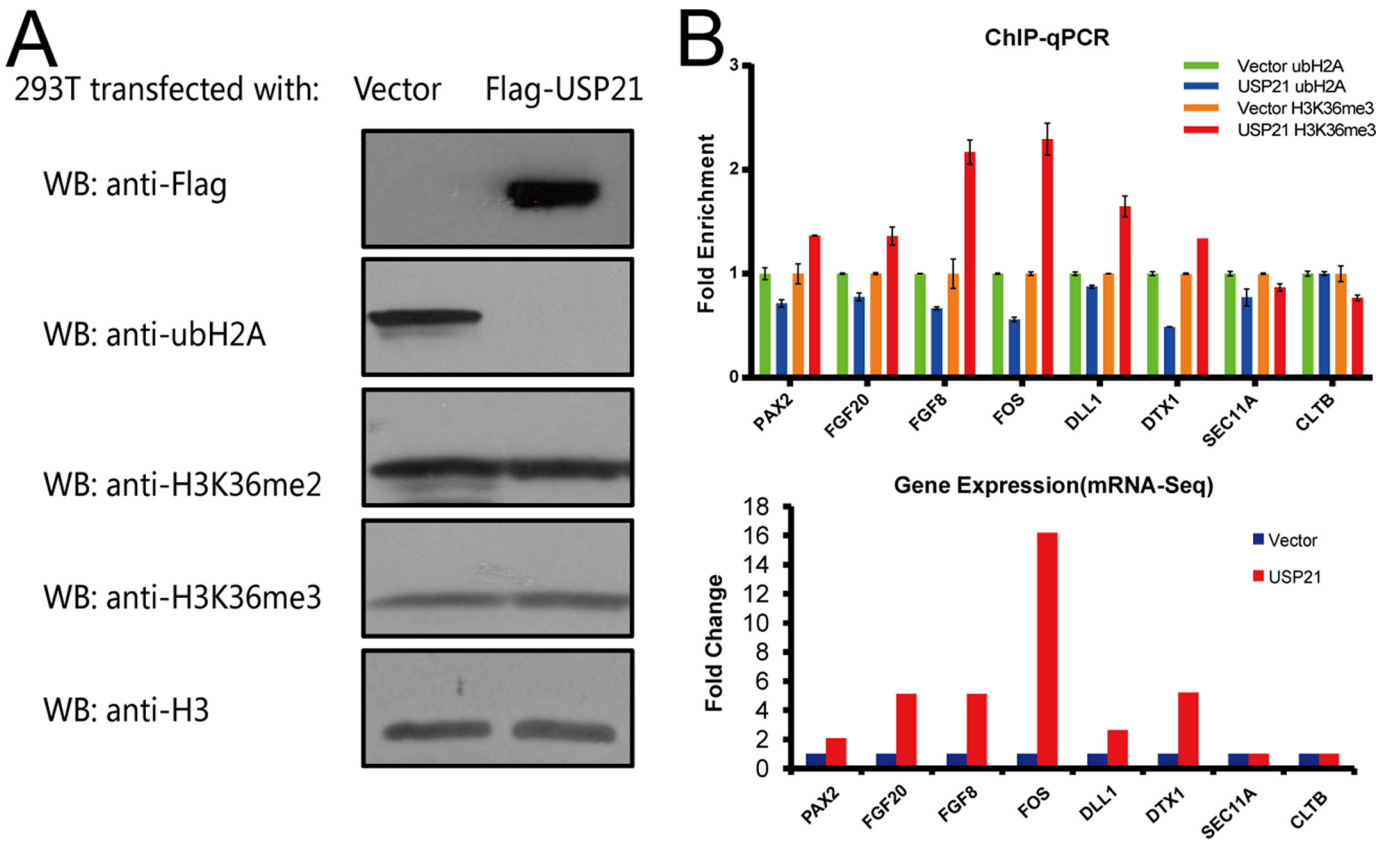

FIGURE 6. **ubH2A down-regulation elevates H3K36me3 at a subset of up-regulated genes.** *A,* overexpression of USP21 down-regulates ubH2A level, but does not alter H3K36me2 or H3K36me3 levels globally. *B,* down-regulation of ubH2A and concomitant elevation of H3K36me3 occur at a subset of up-regulated genes upon USP21 overexpression. *Upper panel*, ChIP-quantitative PCR results for a list of genes. *Lower panel*, mRNA-seq results for the same genes. *WB*, Western blot; qPCR, quantitative PCR.

ubH2A Down-regulation Elevates H3K36me3 at a Subset of Up-regulated Genes—To manipulate the level of ubH2A in cells, USP21 was overexpressed in HEK 293T cells and led to the reduction of global ubH2A level (Fig. 6*A*). However, the global level of H3K36me2 and H3K36me3 were not significantly up-regulated (Fig. 6*A*). This is not totally unexpected, because H3K36me2 and H3K36me3 are quite abundant and accounts for ~30% of total H3 polypeptides in mammalian cells (19, 38).

Then, we performed mRNA-Seq experiments for HEK 293T cells with or without overexpression of USP21. There were ~1000 up-regulated genes and 600 down-regulated genes with more than 2-fold expression changes in cells overexpressing USP21. We chose several of the up-regulated genes and unchanged genes according to our mRNA-Seq data (Fig. 6*B*) and literature (57), and then performed ChIP-quantitative PCR experiments using antibodies against ubH2A or H3K36me3. We observed an increase of H3K36me3 and a concomitant reduction of ubH2A at the most highly up-regulated genes, such as *FOS* and *FGF8* (Fig. 6*B*). Similar but milder changes were observed at some other modestly up-regulated genes, such as *PAX2*, *FGF20*, *DLL1*, and *DTX1* (Fig. 6*B*). These changes were not observed at two unchanged control genes *SEC11A* and *CLTB* (Fig. 6*B*). The above observations do not rule out a secondary effect of H3K36me3 followed by gene induction, but is also consistent with a role of ubH2A down-regulation in up-regulating H3K36 methylation.

DISCUSSION

PcG and TrxG proteins display counteracting functions to maintain the correct expression pattern of developmental regulated genes (30, 59–62). The correct chromatin modification patterns are important transcription regulators of these genes. However, one important and not fully addressed question is the mechanism by which chromatin modifiers set up such modification patterns. Because of the critical role of Polycomb response elements in recruiting the Polycomb group proteins in *Drosophila* (63, 64), and because there are only a few Polycomb response elements identified in mammals (65, 66), alternative recruitment mechanisms, such as non-coding RNA-mediated PRC2 recruitment have been proposed and debated (67–69).

However, many recent progresses support an alternative sensor model, which may function independently and/or in combination with the recruitment model. The central point of the sensor model is that some chromatin modifying enzymes are not merely the robotic modification producers that generate reaction products wherever they get recruited, but instead, they may function as smart enzymes that can sense the chromatin environment and adjust their enzymatic activities accordingly. To date, the best characterized example is H3K27-specific methyltransferase PRC2, which can be negatively regulated by chromatin features associated with active transcription including H3K36 methylation (19, 39), H3K4me3 (39), and open chromatin (44) (Fig. 7). Moreover, PRC2 can also be stimulated by

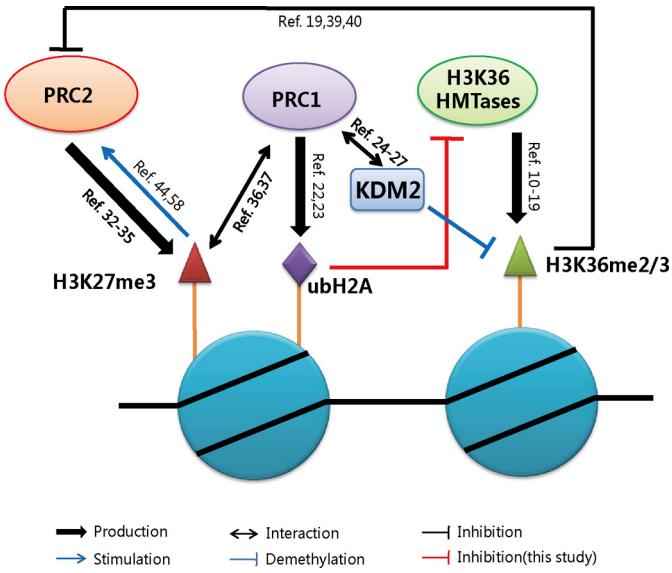

FIGURE 7. **A model of cross-talk between H3K36 methylation and Polycomb modifications.** The results from previous publications are labeled with the reference numbers.

chromatin features associated with silent genes including H3K27me3 (58) and compact chromatin (44) (Fig. 7).

In this study, we observed similar regulatory activities on H3K36-specific methyltransferases by H2A monoubiquitination (Figs. 2–4). H2A monoubiquitination effectively inhibits the enzymatic activity of ASH1L (Figs. 2*A*, 3*A*, and 4*B*), a classic TrxG protein (52–54) that mediates H3K36me2 (17–19). In addition to reporting a new instance of cross-talk between histone modifications, this study also helps to explain the gap between the mutual exclusion between H3K27me3 and H3K36 methylation observed *in vivo* (19, 38) and the previously reported unidirectional inhibition of PRC2 activity by H3K36 methylation (19, 39).

Finally, we would like to share our view of Polycomb regulation. We believe that the distinct transcription states of Polycomb-regulated genes, which are initially determined by sequence-specific transcription factors, establish and determine their characteristic chromatin modification patterns, which in turn reinforce the transcriptional states of their underlying genes.

REFERENCES

1. Wang, Y., Fischle, W., Cheung, W., Jacobs, S., Khorasanizadeh, S., and Allis, C. D. (2004) Beyond the double helix: writing and reading the histone code. *Novartis Found. Symp.* **259,** 3–17; discussion 17–21, 163–169
2. Li, B., Carey, M., and Workman, J. L. (2007) The role of chromatin during transcription. *Cell* **128,** 707–719
3. Kouzarides, T. (2007) Chromatin modifications and their function. *Cell* **128,** 693–705
4. Campos, E. I., and Reinberg, D. (2009) Histones. Annotating chromatin. *Annu. Rev. Genet.* **43,** 559–599
5. Soria, G., Polo, S. E., and Almouzni, G. (2012) Prime, repair, restore. The active role of chromatin in the DNA damage response. *Mol. Cell* **46,** 722–734
6. Musselman, C. A., Lalonde, M. E., Côté, J., and Kutateladze, T. G. (2012) Perceiving the epigenetic landscape through histone readers. *Nat. Struct. Mol. Biol.* **19,** 1218–1227
7. Wagner, E. J., and Carpenter, P. B. (2012) Understanding the language of Lys36 methylation at histone H3. *Nat. Rev. Mol. Cell Biol.* **13,** 115–126
8. Varier, R. A., and Timmers, H. T. (2011) Histone lysine methylation and demethylation pathways in cancer. *Biochim. Biophys. Acta* **1815,** 75–89
9. Strahl, B. D., Grant, P. A., Briggs, S. D., Sun, Z. W., Bone, J. R., Caldwell, J. A., Mollah, S., Cook, R. G., Shabanowitz, J., Hunt, D. F., and Allis, C. D. (2002) Set2 is a nucleosomal histone H3-selective methyltransferase that mediates transcriptional repression. *Mol. Cell Biol.* **22,** 1298–1306
10. Edmunds, J. W., Mahadevan, L. C., and Clayton, A. L. (2008) Dynamic histone H3 methylation during gene induction. HYPB/Setd2 mediates all H3K36 trimethylation. *EMBO J.* **27,** 406–420
11. Sun, X. J., Wei, J., Wu, X. Y., Hu, M., Wang, L., Wang, H. H., Zhang, Q. H., Chen, S. J., Huang, Q. H., and Chen, Z. (2005) Identification and characterization of a novel human histone H3 lysine 36-specific methyltransferase. *J. Biol. Chem.* **280,** 35261–35271
12. Yuan, W., Xie, J., Long, C., Erdjument-Bromage, H., Ding, X., Zheng, Y., Tempst, P., Chen, S., Zhu, B., and Reinberg, D. (2009) Heterogeneous nuclear ribonucleoprotein L Is a subunit of human KMT3a/Set2 complex required for H3 Lys-36 trimethylation activity *in vivo*. *J. Biol. Chem.* **284,** 15701–15707
13. Li, Y., Trojer, P., Xu, C. F., Cheung, P., Kuo, A., Drury, W. J., 3rd, Qiao, Q., Neubert, T. A., Xu, R. M., Gozani, O., and Reinberg, D. (2009) The target of the NSD family of histone lysine methyltransferases depends on the nature of the substrate. *J. Biol. Chem.* **284,** 34283–34295
14. Lucio-Eterovic, A. K., Singh, M. M., Gardner, J. E., Veerappan, C. S., Rice, J. C., and Carpenter, P. B. (2010) Role for the nuclear receptor-binding SET domain protein 1 (NSD1) methyltransferase in coordinating lysine 36 methylation at histone 3 with RNA polymerase II function. *Proc. Natl. Acad. Sci. U.S.A.* **107,** 16952–16957
15. Qiao, Q., Li, Y., Chen, Z., Wang, M., Reinberg, D., and Xu, R. M. (2011) The structure of NSD1 reveals an autoregulatory mechanism underlying histone H3K36 methylation. *J. Biol. Chem.* **286,** 8361–8368
16. Kuo, A. J., Cheung, P., Chen, K., Zee, B. M., Kioi, M., Lauring, J., Xi, Y., Park, B. H., Shi, X., Garcia, B. A., Li, W., and Gozani, O. (2011) NSD2 links dimethylation of histone H3 at lysine 36 to oncogenic programming. *Mol. Cell* **44,** 609–620
17. Tanaka, Y., Katagiri, Z., Kawahashi, K., Kioussis, D., and Kitajima, S. (2007) Trithorax-group protein ASH1 methylates histone H3 lysine 36. *Gene* **397,** 161–168
18. An, S., Yeo, K. J., Jeon, Y. H., and Song, J. J. (2011) Crystal structure of the human histone methyltransferase ASH1L catalytic domain and its implications for the regulatory mechanism. *J. Biol. Chem.* **286,** 8369–8374
19. Yuan, W., Xu, M., Huang, C., Liu, N., Chen, S., and Zhu, B. (2011) H3K36 methylation antagonizes PRC2-mediated H3K27 methylation. *J. Biol. Chem.* **286,** 7983–7989
20. Levinger, L., and Varshavsky, A. (1980) High-resolution fractionation of nucleosomes. Minor particles, "whiskers," and separation of mononucleosomes containing and lacking A24 semihistone. *Proc. Natl. Acad. Sci. U.S.A.* **77,** 3244–3248
21. Böhm, L., Crane-Robinson, C., and Sautière, P. (1980) Proteolytic digestion studies of chromatin core-histone structure. Identification of a limit peptide of histone H2A. *Eur. J. Biochem.* **106,** 525–530
22. Wang, H., Wang, L., Erdjument-Bromage, H., Vidal, M., Tempst, P., Jones, R. S., and Zhang, Y. (2004) Role of histone H2A ubiquitination in Polycomb silencing. *Nature* **431,** 873–878
23. Cao, R., Tsukada, Y., and Zhang, Y. (2005) Role of Bmi-1 and Ring1A in H2A ubiquitylation and *Hox* gene silencing. *Mol. Cell* **20,** 845–854
24. Sánchez, C., Sánchez, I., Demmers, J. A., Rodriguez, P., Strouboulis, J., and Vidal, M. (2007) Proteomics analysis of Ring1B/Rnf2 interactors identifies a novel complex with the Fbxl10/Jhdm1B histone demethylase and the Bcl6 interacting corepressor. *Mol. Cell Proteomics* **6,** 820–834
25. Gearhart, M. D., Corcoran, C. M., Wamstad, J. A., and Bardwell, V. J. (2006) Polycomb group and SCF ubiquitin ligases are found in a novel BCOR complex that is recruited to BCL6 targets. *Mol. Cell. Biol.* **26,** 6880–6889
26. Lagarou, A., Mohd-Sarip, A., Moshkin, Y. M., Chalkley, G. E., Bezstarosti, K., Demmers, J. A., and Verrijzer, C. P. (2008) dKDM2 couples histone H2A ubiquitylation to histone H3 demethylation during Polycomb group silencing. *Genes Dev.* **22,** 2799–2810
27. He, J., Shen, L., Wan, M., Taranova, O., Wu, H., and Zhang, Y. (2013) Kdm2b maintains murine embryonic stem cell status by recruiting PRC1 complex to CpG islands of developmental genes. *Nat. Cell Biol.* **15,** 373–384
28. Zhou, W., Zhu, P., Wang, J., Pascual, G., Ohgi, K. A., Lozach, J., Glass,

C. K., and Rosenfeld, M. G. (2008) Histone H2A monoubiquitination represses transcription by inhibiting RNA polymerase II transcriptional elongation. *Mol. Cell* **29,** 69–80
29. Xia, Y., Pao, G. M., Chen, H. W., Verma, I. M., and Hunter, T. (2003) Enhancement of BRCA1 E3 ubiquitin ligase activity through direct interaction with the BARD1 protein. *J. Biol. Chem.* **278,** 5255–5263
30. Simon, J. A., and Kingston, R. E. (2009) Mechanisms of polycomb gene silencing. Knowns and unknowns. *Nat. Rev. Mol. Cell Biol.* **10,** 697–708
31. Zhu, Q., Pao, G. M., Huynh, A. M., Suh, H., Tonnu, N., Nederlof, P. M., Gage, F. H., and Verma, I. M. (2011) BRCA1 tumour suppression occurs via heterochromatin-mediated silencing. *Nature* **477,** 179–184
32. Müller, J., Hart, C. M., Francis, N. J., Vargas, M. L., Sengupta, A., Wild, B., Miller, E. L., O'Connor, M. B., Kingston, R. E., and Simon, J. A. (2002) Histone methyltransferase activity of a *Drosophila* Polycomb group repressor complex. *Cell* **111,** 197–208
33. Czermin, B., Melfi, R., McCabe, D., Seitz, V., Imhof, A., and Pirrotta, V. (2002) *Drosophila* enhancer of Zeste/ESC complexes have a histone H3 methyltransferase activity that marks chromosomal Polycomb sites. *Cell* **111,** 185–196
34. Cao, R., Wang, L., Wang, H., Xia, L., Erdjument-Bromage, H., Tempst, P., Jones, R. S., and Zhang, Y. (2002) Role of histone H3 lysine 27 methylation in Polycomb-group silencing. *Science* **298,** 1039–1043
35. Kuzmichev, A., Nishioka, K., Erdjument-Bromage, H., Tempst, P., and Reinberg, D. (2002) Histone methyltransferase activity associated with a human multiprotein complex containing the Enhancer of Zeste protein. *Genes Dev.* **16,** 2893–2905
36. Schwartz, Y. B., Kahn, T. G., Nix, D. A., Li, X. Y., Bourgon, R., Biggin, M., and Pirrotta, V. (2006) Genome-wide analysis of Polycomb targets in *Drosophila melanogaster*. *Nat. Genet.* **38,** 700–705
37. Boyer, L. A., Plath, K., Zeitlinger, J., Brambrink, T., Medeiros, L. A., Lee, T. I., Levine, S. S., Wernig, M., Tajonar, A., Ray, M. K., Bell, G. W., Otte, A. P., Vidal, M., Gifford, D. K., Young, R. A., and Jaenisch, R. (2006) Polycomb complexes repress developmental regulators in murine embryonic stem cells. *Nature* **441,** 349–353
38. Young, N. L., DiMaggio, P. A., Plazas-Mayorca, M. D., Baliban, R. C., Floudas, C. A., and Garcia, B. A. (2009) High throughput characterization of combinatorial histone codes. *Mol. Cell Proteomics* **8,** 2266–2284
39. Schmitges, F. W., Prusty, A. B., Faty, M., Stützer, A., Lingaraju, G. M., Aiwazian, J., Sack, R., Hess, D., Li, L., Zhou, S., Bunker, R. D., Wirth, U., Bouwmeester, T., Bauer, A., Ly-Hartig, N., Zhao, K., Chan, H., Gu, J., Gut, H., Fischle, W., Müller, J., and Thomä, N. H. (2011) Histone methylation by PRC2 is inhibited by active chromatin marks. *Mol. Cell* **42,** 330–341
40. Voigt, P., LeRoy, G., Drury, W. J., 3rd, Zee, B. M., Son, J., Beck, D. B., Young, N. L., Garcia, B. A., and Reinberg, D. (2012) Asymmetrically modified nucleosomes. *Cell* **151,** 181–193
41. Shechter, D., Dormann, H. L., Allis, C. D., and Hake, S. B. (2007) Extraction, purification and analysis of histones. *Nat. Protoc.* **2,** 1445–1457
42. Xu, M., Long, C., Chen, X., Huang, C., Chen, S., and Zhu, B. (2010) Partitioning of histone H3-H4 tetramers during DNA replication-dependent chromatin assembly. *Science* **328,** 94–98
43. Chen, X., Xiong, J., Xu, M., Chen, S., and Zhu, B. (2011) Symmetrical modification within a nucleosome is not required globally for histone lysine methylation. *EMBO Rep.* **12,** 244–251
44. Yuan, W., Wu, T., Fu, H., Dai, C., Wu, H., Liu, N., Li, X., Xu, M., Zhang, Z., Niu, T., Han, Z., Chai, J., Zhou, X. J., Gao, S., and Zhu, B. (2012) Dense chromatin activates Polycomb repressive complex 2 to regulate H3 lysine 27 methylation. *Science* **337,** 971–975
45. Jia, G., Wang, W., Li, H., Mao, Z., Cai, G., Sun, J., Wu, H., Xu, M., Yang, P., Yuan, W., Chen, S., and Zhu, B. (2009) A systematic evaluation of the compatibility of histones containing methyl-lysine analogues with biochemical reactions. *Cell Res.* **19,** 1217–1220
46. Kallin, E. M., Cao, R., Jothi, R., Xia, K., Cui, K., Zhao, K., and Zhang, Y. (2009) Genome-wide uH2A localization analysis highlights Bmi1-dependent deposition of the mark at repressed genes. *PLoS Genet.* **5,** e1000506
47. Mikkelsen, T. S., Ku, M., Jaffe, D. B., Issac, B., Lieberman, E., Giannoukos, G., Alvarez, P., Brockman, W., Kim, T. K., Koche, R. P., Lee, W., Mendenhall, E., O'Donovan, A., Presser, A., Russ, C., Xie, X., Meissner, A., Wernig, M., Jaenisch, R., Nusbaum, C., Lander, E. S., and Bernstein, B. E. (2007) Genome-wide maps of chromatin state in pluripotent and lineage-committed cells. *Nature* **448,** 553–560
48. McGinty, R. K., Kim, J., Chatterjee, C., Roeder, R. G., and Muir, T. W. (2008) Chemically ubiquitylated histone H2B stimulates hDot1L-mediated intranucleosomal methylation. *Nature* **453,** 812–816
49. Fierz, B., Kilic, S., Hieb, A. R., Luger, K., and Muir, T. W. (2012) Stability of nucleosomes containing homogenously ubiquitylated H2A and H2B prepared using semisynthesis. *J. Am. Chem. Soc.* **134,** 19548–19551
50. Whitcomb, S. J., Fierz, B., McGinty, R. K., Holt, M., Ito, T., Muir, T. W., and Allis, C. D. (2012) Histone monoubiquitylation position determines specificity and direction of enzymatic cross-talk with histone methyltransferases Dot1L and PRC2. *J. Biol. Chem.* **287,** 23718–23725
51. Hunter, A. J., and Cary, P. D. (1985) Preparation of chromosomal protein A24 (uH2A) by denaturing gel filtration and preparation of its free non-histone component ubiquitin by ion-exchange chromatography. *Anal. Biochem.* **150,** 394–402
52. Shearn, A. (1989) The *ash-1*, *ash-2,* and *trithorax* genes of *Drosophila melanogaster* are functionally related. *Genetics* **121,** 517–525
53. Klymenko, T., and Müller, J. (2004) The histone methyltransferases Trithorax and Ash1 prevent transcriptional silencing by Polycomb group proteins. *EMBO Rep.* **5,** 373–377
54. Schwartz, Y. B., Kahn, T. G., Stenberg, P., Ohno, K., Bourgon, R., and Pirrotta, V. (2010) Alternative epigenetic chromatin states of polycomb target genes. *PLoS Genet.* **6,** e1000805
55. Nakagawa, T., Kajitani, T., Togo, S., Masuko, N., Ohdan, H., Hishikawa, Y., Koji, T., Matsuyama, T., Ikura, T., Muramatsu, M., and Ito, T. (2008) Deubiquitylation of histone H2A activates transcriptional initiation via trans-histone cross-talk with H3K4 di- and trimethylation. *Genes Dev.* **22,** 37–49
56. Bannister, A. J., Schneider, R., Myers, F. A., Thorne, A. W., Crane-Robinson, C., and Kouzarides, T. (2005) Spatial distribution of di- and tri-methyl lysine 36 of histone H3 at active genes. *J. Biol. Chem.* **280,** 17732–17736
57. Bracken, A. P., Dietrich, N., Pasini, D., Hansen, K. H., and Helin, K. (2006) Genome-wide mapping of Polycomb target genes unravels their roles in cell fate transitions. *Genes Dev.* **20,** 1123–1136
58. Margueron, R., Justin, N., Ohno, K., Sharpe, M. L., Son, J., Drury, W. J., 3rd, Voigt, P., Martin, S. R., Taylor, W. R., De Marco, V., Pirrotta, V., Reinberg, D., and Gamblin, S. J. (2009) Role of the polycomb protein EED in the propagation of repressive histone marks. *Nature* **461,** 762–767
59. Schuettengruber, B., Martinez, A. M., Iovino, N., and Cavalli, G. (2011) Trithorax group proteins. Switching genes on and keeping them active. *Nat. Rev. Mol. Cell Biol.* **12,** 799–814
60. Whitcomb, S. J., Basu, A., Allis, C. D., and Bernstein, E. (2007) Polycomb Group proteins. An evolutionary perspective. *Trends Genet.* **23,** 494–502
61. Kerppola, T. K. (2009) Polycomb group complexes. Many combinations, many functions. *Trends Cell Biol.* **19,** 692–704
62. Schwartz, Y. B., and Pirrotta, V. (2007) Polycomb silencing mechanisms and the management of genomic programmes. *Nat. Rev. Genet.* **8,** 9–22
63. Müller, J., and Kassis, J. A. (2006) Polycomb response elements and targeting of Polycomb group proteins in *Drosophila*. *Curr. Opin. Genet. Dev.* **16,** 476–484
64. Ringrose, L., and Paro, R. (2007) Polycomb/Trithorax response elements and epigenetic memory of cell identity. *Development* **134,** 223–232
65. Woo, C. J., Kharchenko, P. V., Daheron, L., Park, P. J., and Kingston, R. E. (2010) A region of the human HOXD cluster that confers polycomb-group responsiveness. *Cell* **140,** 99–110
66. Sing, A., Pannell, D., Karaiskakis, A., Sturgeon, K., Djabali, M., Ellis, J., Lipshitz, H. D., and Cordes, S. P. (2009) A vertebrate Polycomb response element governs segmentation of the posterior hindbrain. *Cell* **138,** 885–897
67. Brockdorff, N. (2013) Noncoding RNA and Polycomb recruitment. *Rna* **19,** 429–442
68. Lee, J. T., Strauss, W. M., Dausman, J. A., and Jaenisch, R. (1996) A 450 kb transgene displays properties of the mammalian X-inactivation center. *Cell* **86,** 83–94
69. Rinn, J. L., Kertesz, M., Wang, J. K., Squazzo, S. L., Xu, X., Brugmann, S. A., Goodnough, L. H., Helms, J. A., Farnham, P. J., Segal, E., and Chang, H. Y. (2007) Functional demarcation of active and silent chromatin domains in human HOX loci by noncoding RNAs. *Cell* **129,** 1311–1323